LAWRENCE
LIVERMORE
NATIONAL
LABORATORY

LLNL-CONF-425269

Three-Dimensional Magnetohydrodynamic Simulation of Slapper Initiation Systems

J. S. Christensen, C. A. Hrousis

March 9, 2010

14th International Detonation Symposium
Coeur d'Alene, ID, United States
April 11, 2010 through April 16, 2010

Disclaimer

Three-Dimensional Magnetohydrodynamic Simulation of Slapper Initiation Systems

John S. Christensen and Constantine A. Hrousis

Defense Technologies Engineering Division
Lawrence Livermore National Laboratory, Livermore, CA, 94550

Abstract. Although useful information can be gleaned from 2D and even 1D simulations of slapper type initiation systems, these systems are inherently three-dimensional and therefore require full 3D representation to model all relevant details. Further, such representation provides additional insight into optimizing the design of such devices from a first-principles perspective and can thereby reduce experimental costs. We discuss in this paper several ongoing efforts in modeling these systems, our pursuit of validation, and extension of these methods to other systems. Our results show the substantial dependence upon highly accurate global equations of state and resistivity models in these analyses.

Introduction

Many initiation systems utilize rapid electrical energy deposition into thin metal foils which then vaporize and thereby accelerate an inert plastic flyer plate across some distance into a high explosive (HE) material. Detonators utilizing these processes are commonly known as slapper-type initiation systems. Characterization of such a system requires extensive empirical efforts to determine optimal initial bridgefoil and slapper geometry and threshold initiation criteria such as initial charge voltage. Additional characterizations of the dynamic function of such devices are also often pursued; e.g., flyer velocity profile, flyer geometry at impact, pulse duration, etc. Although measurements and diagnostics for these systems continue to improve, a detailed first-principles understanding of all the combined relevant physics has not yet been achieved. Three-dimensional computational simulation of these systems provides additional insight into phenomena that is difficult to observe experimentally. Electromagnetic phenomena such as current diffusion into a conductor from the skin inward as the current density builds or even prediction of the dynamically varying current path are readily visualized with this approach. As the current density builds and eventually explodes the rectangular bridgefoil, the slapper material is then generally driven through a cylindrical barrel – an effect that cannot be well represented in 2D. Further, flyer geometry can be predicted at each stage as it (1) forms due to the expanding bridgefoil plasma, (2) traverses some distance toward the initiating HE while deforming and ablating, and (3) as the slapper impacts the first stage HE pressing or pellet.

In this document, we discuss our ongoing efforts in modeling the influential aspects of these systems. In so doing, we discuss several slapper-type initiation systems from very large (25.4 x

25.4 x 0.254mm) to very small (203.2 x 203.2 x 12.5µm) flyers in terms of model validation to empirical data as well as extension to similar systems.

Experiments

For our "very large" slapper initiation efforts, we utilize a multi kilo-joule (up to 44.8kJ) capacitor bank called the electric gun (or "E-gun"). The electric gun is designed to explode large bridgefoils to drive large area flyers at a range of velocities. The ultimate purpose of this series of experiments was to better determine the initiation threshold of UF-TATB.

Both the bridgefoils and flyers are mounted on prefabricated laminates, each of which is approximately 300mm long and 76.2mm wide. Each laminate consists of 0.127mm thick copper conductors that attach to a 0.0508mm thick aluminum bridgefoil that can vary in square cross-section from 3.175mm to 25.4mm to match the intended slapper dimensions (Figure 1). A Mylar flyer is laminated over the bridgefoil, and the entire laminate is then sandwiched between two polycarbonate plates. The bridge region is aligned with a hole in the top plate which clips the Mylar flyer to yield a 12.7mm diameter circular cutout. This clipped slapper then traverses the polycarbonate barrel length prior to impacting the flat side of a 38.1mm diameter hemisphere of UF-TATB. Initiation of the HE was determined by visual inspection of the top polycarbonate plate.

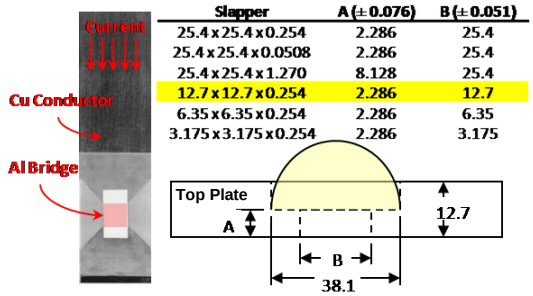

Slapper	A (± 0.076)	B (± 0.051)
25.4 x 25.4 x 0.254	2.286	25.4
25.4 x 25.4 x 0.0508	2.286	25.4
25.4 x 25.4 x 1.270	8.128	25.4
12.7 x 12.7 x 0.254	2.286	12.7
6.35 x 6.35 x 0.254	2.286	6.35
3.175 x 3.175 x 0.254	2.286	3.175

Figure 1: Electric gun schematic showing a laminate (left) and series of slapper / bridgefoil variations used for experiments (right). All results shown for this paper are for the highlighted 12.7 x 12.7 x 0.254mm case. Note that all dimensions shown are in millimeters.

Diagnostic results for the electric gun experiments include current vs. time traces via a current viewing resistor (CVR); bridge burst time as indicated by an un-calibrated Rogowski coil (idot signal); and for non-HE shots, flyer velocity as indicated by Photonic Doppler Velocimetry (PDV)[1].

The "very small" chip-slappers referred to above are 203.2 x 203.2 x 12.5µm Kapton flyers propelled by exploding aluminum or copper bridges of the same length and width varying in thickness from 1.75 to 3.25µm. The bridge material is deposited onto a substrate, followed by deposition of a gold "over-plate" layer to serve as the conductor leading up to the bridge. This geometry is then coated via MEMS processes with Kapton for the flyer material. The polycarbonate barrel diameter for these devices is 800µm, which is large enough relative to the bridge / flyer dimensions to be considered an "infinite" barrel design (as if the barrel were not present). The slapper traverses the 600µm long barrel and a 25µm gap prior to impacting an LX-16 (96% PETN) pellet. The goal of this set of experiments was essentially design optimization, considering specifically the manufacturing tolerance limitations that are particularly influential at that small scale. Measurements for this set of experiments include flyer velocity profiles via PDV as well as both current and voltage vs. time waveforms.

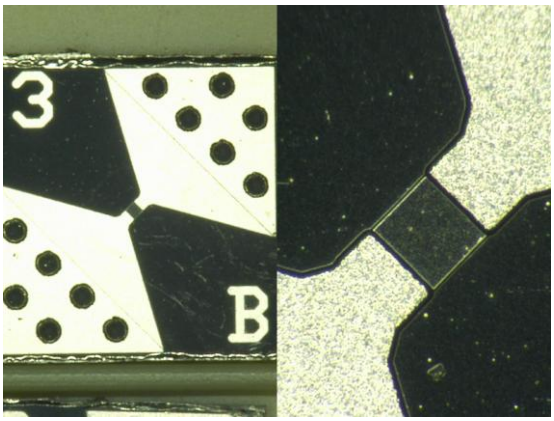

Figure 2: Picture of typical chip-slapper device.

In terms of size, the "bluelite" device shown in Figure 3 utilizes an electrically initiated flyer in its initial stage that is in between the aforementioned systems. The copper bridgefoil is 635 x 635 x 4µm. Explosion of this foil pushes the 50.8µm thick flyer through a 760µm diameter, 457µm long steel barrel and across a 650µm gap to initiate an LX-16 pellet. This pellet then detonates and throws the aluminum "can" that contains the LX-16 into a shearing plate which forms a second stage flyer. Depending on the type of test, this second stage flyer may then impact a booster pellet of UF-TATB.

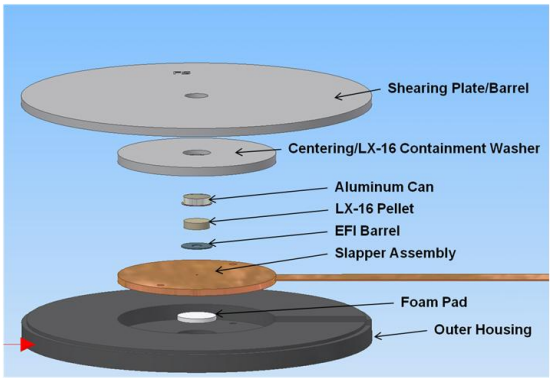

Figure 3: Exploded view schematic of the mid-size, bluelite device[2].

Model Descriptions

Each of these experiments has been modeled utilizing the fully coupled magnetohydrodynamics (MHD) capability that exists in LLNL-developed hydrocode ALE3D to simulate the transformation of electrical energy into the high explosive initiating energy. In each case, energy was deposited into the bridge by way of a simulated equivalent RLC circuit. Each set of simulated fireset parameters was computed from ringdown data on the physical circuit associated with each experiment.

During the function of these devices, the bridgefoil material transitions from solid to liquid to vapor and eventually becomes an electrically conductive plasma. Formulating an equation of state (EOS) that is applicable over such a large range is a significant challenge in accurately modeling this process. Further, the electrical resistance of the bridge is dynamically changing during these transitions as a function of temperature and density which are also driven by the material EOS. For these reasons, tabular equations of state (LEOS or Sesame) were generally utilized as they define the material state across this entire range. However, the accuracy of each table can vary substantially and they are generally not amenable to non-uniform alteration to improve known regions of greater error (can result in loss of thermodynamic consistency). An alternative analytical EOS, GRAY[3], was also utilized due to the relative flexibility in terms of modification as well as its ability to explicitly include relevant physics such as latent heats of fusion and vaporization. Similarly, the electrical conductivity model must also maintain an acceptable level of accuracy over these transitions. In all analyses presented here, tabular conductivities were used as described elsewhere[4].

Steinberg-Guinan strength models[5] were utilized for most metals and some polymers (where available). The Kapton / Mylar flyer materials were represented by tabular equations of state (LEOS) and simpler strength models such as constant yield strength and shear modulus or bilinear forms. All meshes were generated using TrueGrid, Cubit, or ALE3D's internal mesh generator.

Results and Discussion

As stated above, common validation metrics for each of these simulations include current waveforms and flyer velocity. In our efforts to validate these simulations we have exposed several modeling needs that we believe can be resolved in the relatively near future. Specifically, in comparing predictions of flyer velocity and current waveforms with electric gun empirical data we have determined several factors that are highly influential in simulation of these systems. From Figure 4, it is evident that our models do not accurately predict the measured current. Since the current is essentially the excitation of the system it should be anticipated that this error will also influence bridge burst phenomena such as material expansion and therefore flyer velocity. Figure 4 also shows the effect of alterations to the

simulation in terms of equation of state and circuit parameters. The inaccuracy in the initial slope of the current rise observed in both simulations that utilize the ringdown characterized circuit parameters indicates our model is in error with either initial charge voltage or inductance; i.e., the simulated rise time is higher than the data (from $\delta=V_0/L$). This indicates that either our initial charge voltage is too high or the inductance measurement is too low for the system as we have modeled it. In contrast, inaccuracies after the initial current rise indicate we are likely in error with either the resistance or capacitance. Therefore, the "adjusted" version as shown in Figure 4 is an attempt to better match the measured waveform by adjusting inductance and resistance within the experimental uncertainty for these metrics. The assumptions are that the charge voltage and capacitance as measured are accurate and that our model could be missing influential components in efforts to maintain computational efficiency. The adjusted parameters do improve the fit to data as shown but could likely further benefit from a more rigorous attempt.

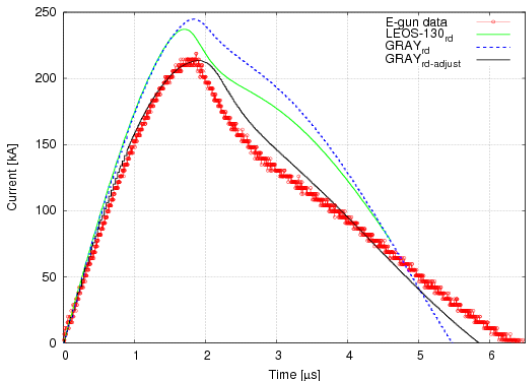

Figure 4: Electric gun experimental and simulated current vs. time waveforms for the 12.7 x 12.7 x 0.254mm foil geometry. Note the "rd" subscript to identify the circuit parameters as determined from ringdown data.

In terms of flyer velocity predictions, all E-gun simulations over-predict the PDV data. In addition to the variations shown in Figure 4, Figure 5 shows the predicted flyer velocity using the measured current as the simulation input instead of the circuit model for each EOS. This is intended to illustrate the extent to which the equation of state influences the calculation. As shown, using the measured current over-predicts the maximum flyer velocity by approximately 5% using the GRAY EOS for the aluminum bridge. Although the timing is off[a] with this variation, the velocity trace tracks more closely with the data than it does with the QEOS-based LEOS-130 calculation.

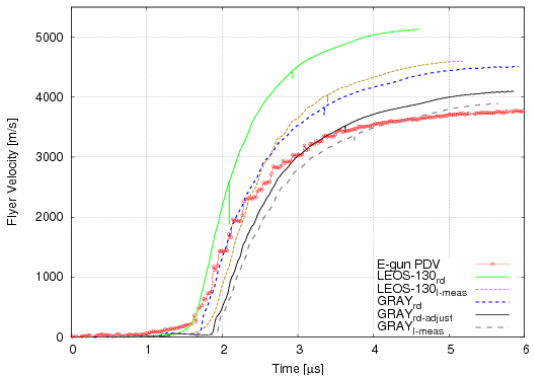

Figure 5: Electric gun experimental and simulated flyer velocity vs. time for several different simulations. Note that the start time for the PDV is unknown and was therefore shifted in time to approximately match simulations.

It is apparent from this comparison that the GRAY equation of state produces pressures in this regime (less than approximately 20,000K) that are much closer to the experiment than LEOS-130. Further, QEOS-based[6,7] equations of state have been shown to produce higher pressures than are observed experimentally[8]. The GRAY EOS as utilized in this series of studies is based on physical values where they are available (latent heats, Hugoniot, liquid density, etc.). However, its formulation does enable greater ability to "tune" behavior should it be necessary to match empirical evidence, which could be a desirable attribute.

One substantial advantage of the chip-slapper data over the electric gun is the addition of a

[a] Evident from the variation in observed vs. simulated inflection points in the current vs. time trace post-peak which generally coincides with burst time.

voltage vs. time trace. Since the voltage trace is strong indicator of the bridge resistance it provides a significant point of validation in terms of both the equation of state and the resistivity model. That is, if the current is modeled well but the voltage does not match the observed waveform, it is an indicator that the resistivity model is another potential inaccuracy. However, if it both the current and voltage traces are accurately predicted, it provides some validation of the resistivity model (or at least the coupling of the EOS and resistivity models). Figure 6 shows a comparison of measured voltage and current to simulated values using the GRAY equation of state for the chip-slapper analyses. Note specifically the enormous variation between the measured and predicted waveforms that utilize the fireset parameters as computed from ringdown characterizations. The initial slope of the simulated fireset is approximately four times higher than the observed current trace. As was discussed above, this indicates either an inaccurate initial voltage or that our model is missing some inductance compared to the physical setup. As shown in Figure 7, this inaccuracy contributes to a significant error in flyer velocity prediction. We have therefore resolved to use the measured current as the analysis input for further chip-slapper predictions presented here.

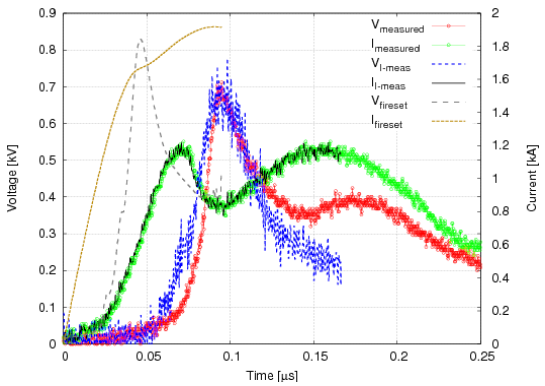

Figure 6: Observed and simulated electrical waveforms for chip-slapper geometry. The subscript "I-meas" indicates that the measured current was used as the analysis input while "fireset" indicates the simulated RLC circuit using ringdown computed parameters.

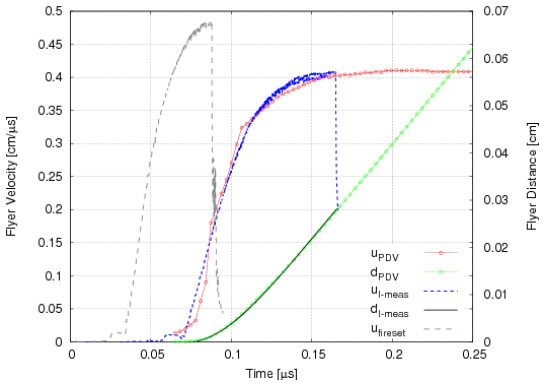

Figure 7: Observed and simulated slapper velocity and position vs. time waveforms. Note that the drop in simulated velocity is due to impact with the HE impact surface.

As shown in Figure 6, using the measured current as the input to the chip-slapper analysis yields remarkable agreement with both voltage and flyer velocity predictions. Although Figure 6 shows some variation with the data as the voltage ramps up and slopes down, a comparison of peak magnitude and burst timing[b] indicates that the coupling of the GRAY equation of state with the resistivity model captures the influential physics reasonably well. This assessment is further confirmed by the flyer velocity and position predictions, which track extremely well with the measured data as shown in Figure 7.

These models have since been used to investigate the effect of manufacturing tolerances on device performance. The current methods for manufacturing these devices can result in substantial variation in the final product from lot to lot. Specifically, a variation of ±15% in both the initial bridgefoil and flyer thicknesses were independently simulated. Since our interest is in the *effect* of these variations as opposed to the absolute prediction of performance, we utilized the simulated fireset with empirically characterized parameters. Although this was shown to result in

[b] Burst time is generally defined as the time of peak resistance in the bridge. Since peak resistance and peak voltage typically coincide in time and voltage is more commonly measured, the voltage peak often defines this metric.

significant error in our validation efforts (Figure 6 Figure 7, this method does indicate the *relative* effect of tolerance deviations from a nominally dimensioned device. Further, since the bridgefoil geometry influences the current waveform, it would also be inaccurate (in an absolute sense) to utilize a measured waveform from a different bridgefoil.

The output metric for this study was flyer velocity at the time the slapper impacts the nearby HE material (625μm total traverse distance). Note that for the bridgefoil thickness variations, the burst time is also altered; i.e., thinner foils burst sooner but have less volume to excite and expand for a given energy input. Utilizing a metric based on the maximum speed achieved over a given distance instead of maximum possible flyer velocity therefore yields a more useful comparison with regard to actual application. For a given energy input (i.e., the same fireset), it was determined that the flyer thickness was more influential than foil thickness (Table 1). These simulations illustrate the potential savings in time and effort relative to experimental iteration. With the initial effort expended to create and validate the model, expanding this "numerical experiment" to a larger test matrix is trivial.

Table 1: Chip-slapper simulated initial geometry variations and the effect on flyer speed at impact.

Thickness	Percent Change in Speed at Impact	
[%]	Bridge [%]	Flyer [%]
+15	+2.3	-5.2
-15	-2.9	+5.2

With regard to the bluelite device, validation data was limited to flyer velocity at several different fireset conditions (Table 2). Also, unlike the other two cases discussed above, the bridgefoil material is copper. As a result, this study provides a somewhat weaker validation of our model input in that we are less capable of attributing error to specific components of the analysis; e.g. the equation of state and/or the resistivity model. Instead, we merely determine the quality of the combination of model input without a clear avenue toward improvement. Improved validation tests are in progress.

Table 2: Experimental firing conditions and resulting maximum flyer velocities. Estimated resistance and inductance were 100mΩ and 60nH, respectively.

Capacitance	Voltage	Flyer Velocity
[μF]	[kV]	[m/s]
0.29	2.5	3200
2.32	2.0	3950
2.32	3.5	4560

As shown in Figure 8, the calculated flyer velocity is not in good agreement with the empirical data. The velocities shown are for the first set of fireset parameters indicated in Table 2 and are typical of all calculated results. The significant over-predictions (greater than 20%) are indicative of either (1) an excess of energy into the system or (2) inaccuracies resulting from the combination of EOS and resistivity models – particularly of the bridgefoil. As alluded to above for the electric gun experiments, an excess of energy or even rate of energy deposition could be assessed to some extent with current and voltage waveforms, neither of which are available for this set of experiments. Similarly, it is difficult to attribute error independently to either the EOS or resistivity models without additional information. It is apparent though that the combination of all components of the analysis yield higher pressures thereby driving the slapper to faster velocities than were observed in the experiments. It is also of note that while neither LEOS-290 nor the GRAY equation of state adequately represents the data, GRAY again generates phenomena closer to observations than the QEOS-based table.

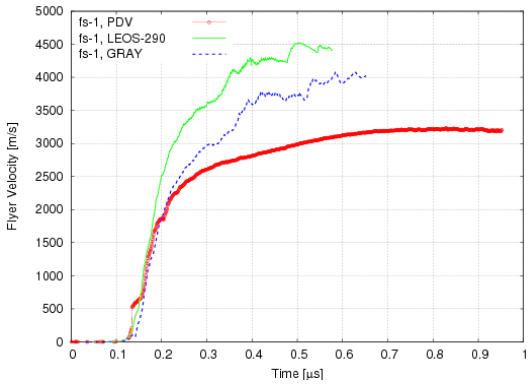

Figure 8: Flyer velocity compared to calculations with different equations of state.

Another attractive aspect of full three-dimensional modeling is visualization of the slapper formation and traversal process. For this data set, sufficient data does not exist for a rigorous quantitative validation so we instead make a purely qualitative comparison within our modeling assumptions. Although material strength is not highly influential in terms of flyer velocity, Figure 9 shows the variation in slapper shape resulting from using a simple strain based failure model compared with no failure model. For the strain based failure model, when the plastic strain exceeds a user defined threshold, that material is considered failed and is then only allowed to sustain hydrostatic pressure (i.e., deviatoric stresses are set to zero). As shown, the analysis with the failure model yields a thicker, more uniform slapper and results in a cleaner break from the parent material. However, the analysis without the failure model shows a thinner flyer from being stretched more during formation in the barrel and it is breaking up sooner. All of these phenomena will have an effect on initiation of the nearby explosive. These variations indicate an additional need for more accurate characterizations of slapper materials.

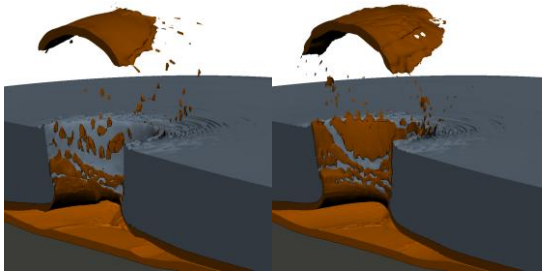

Figure 9: Simulated flyer geometry near impact time with the LX-16 pellet using a simple strain based failure model (left) vs. without a failure model (right). The plasma and surrounding materials have been removed to better visualize the flyer.

Conclusions

Our results illustrate our progress in developing methods for three-dimensional magnetohydrodynamic analyses of slapper type initiation systems. We have discussed several studies that have provided useful information toward improving our modeling techniques and assumptions. Specifically, we have validated certain influential components of our analyses for these problems and further demonstrated areas that require additional effort. For all cases discussed above, the coupled influence of the equation of state and resistivity models has been the dominant factor in reproducing observed output metrics. Continuing efforts will be focused on development and validation of high accuracy global equations of state for relevant bridgefoil materials as well as more accurate general characterization and modeling of slapper materials.

Prepared by LLNL under Contract DE-AC52-07NA27344.

References

1. Davis, R.W., “Probabilistic Threshold of Ultrafine-TATB Using the LLNL Electric Gun” *LLNL Report CODTU-2007-2063*, 2007.

2. May, C.M. and Souers, P.C. “Detonators” in *LLNL Explosives Reference Guide (October 2009) LLNL-WEB-417891*, 2009.

3. Royce, E.B., "GRAY, a Three-Phase Equation of State for Metals" *LLNL Report UCRL-51121*, September 1971.

4. Desjarlais, M.P., Kress, J.D, and Collins, L.A., "Electrical Conductivity for Warm, Dense Aluminum Plasmas and Liquids" *Phys. Rev.* E 66 025401(R), 2002.

5. Steinberg, D.J., "Equation of State and Strength Properties of Selected Materials" *LLNL Report UCRL-MA-106439*, 1996.

6. More, R.M., Warren, K.H., Young, D.A., and Zimmerman, G.B., "A New Quotidian Equation of State (QEOS) for Hot Dense Matter" *Phys. Fluids* 31 (10), October 1988.

7. Young, D.A. and Corey, E.M., "A New Global Equation of State Model for Hot, Dense Matter" *J. Appl. Phys.* 78 (6), September 1995.

8. Renaudin, P., Blancard, C., Clérouin, J., Faussurier, G., Noiret, P., and Recoiles, V., "Aluminum Equation-of-State Data in the Warm Dense Matter Regime" *Phys. Rev. Lett.* 91 (7) 075002, August 2003.